



**University of
Zurich**^{UZH}

**Zurich Open Repository and
Archive**

University of Zurich
University Library
Strickhofstrasse 39
CH-8057 Zurich
www.zora.uzh.ch

Year: 2021

Living Long and Prosperous: Productive Intraligand Charge-Transfer States from a Rhenium(I) Terpyridine Photosensitizer with Enhanced Light Absorption

Fernandez-Teran, Ricardo ; Sévery, Laurent

Abstract: The ground- and excited-state properties of six rhenium(I) 2N-tricarbonyl complexes with 4-(4-substituted-phenyl)terpyridine ligands bearing substituents of different electron-donating abilities were evaluated. Significant modulation of the electrochemical potentials and a nearly 4-fold variation of the triplet metal-to-ligand charge-transfer (3MLCT) lifetimes were observed upon going from CN to OMe. With the more electron-donating NMe₂ group, we observed in the 2N complex the appearance of a very strong absorption band, red-shifted by ca. 100 nm with respect to the other complexes. This was accompanied by a dramatic enhancement of the excited-state lifetime (380 vs 1.5 ns), and a character change from 3MLCT to intraligand charge transfer (3ILCT), despite the remote location of the substituent. The dynamics and character of the excited states of all complexes were assigned by combining transient IR spectroscopy, IR spectroelectrochemistry, and (time-dependent) density functional theory calculations. Selected complexes were evaluated as photosensitizers for hydrogen production, with the 2N-NMe₂ complex resulting in a stable and efficient photocatalytic system reaching TON_{Re} values of over 2100, representing the first application of the 3ILCT state of a rhenium(I) carbonyl complex in a stable photocatalytic system.

DOI: <https://doi.org/10.1021/acs.inorgchem.0c01939>

Posted at the Zurich Open Repository and Archive, University of Zurich

ZORA URL: <https://doi.org/10.5167/uzh-198699>

Journal Article

Accepted Version

Originally published at:

Fernandez-Teran, Ricardo; Sévery, Laurent (2021). Living Long and Prosperous: Productive Intraligand Charge-Transfer States from a Rhenium(I) Terpyridine Photosensitizer with Enhanced Light Absorption. *Inorganic Chemistry*, 60(3):1334-1343.

DOI: <https://doi.org/10.1021/acs.inorgchem.0c01939>

Living Long and Prosperous: Productive Intraligand Charge-Transfer States from a Re(I) Terpyridine Photosensitiser with Enhanced Light Absorption

Ricardo Fernández-Terán* and Laurent Sévery

Department of Chemistry, University of Zurich. Winterthurerstrasse 190, Zurich, Switzerland

*Corresponding Author: Ricardo.Fernandez@chem.uzh.ch

(Dated: August 28, 2020)

Abstract: The ground- and excited-state properties of six Re(I) κ^2N -tricarbonyl complexes with 4'-(4-substituted-phenyl)-terpyridine ligands bearing substituents of different electron donating abilities were evaluated. Significant modulation of the electrochemical potentials and a nearly fourfold variation of the triplet metal-to-ligand charge transfer ($^3\text{MLCT}$) lifetimes were observed when going from CN to OMe. With the more electron-donating NMe₂ group, we observed in the κ^2N complex the appearance of a very strong absorption band, red shifted by ca. 100 nm with respect to the other complexes. This was accompanied by a dramatic enhancement of the excited-state lifetime (380 ns vs 1.5 ns), and a character change from $^3\text{MLCT}$ to intraligand charge transfer ($^3\text{ILCT}$), despite the remote location of the substituent. The dynamics and characters of the excited states of all complexes were assigned by combining transient IR spectroscopy, IR spectroelectrochemistry and (TD-)DFT calculations. Selected complexes were evaluated as photosensitisers for hydrogen production, with the κ^2N -NMe₂ complex resulting in a stable and efficient photocatalytic system reaching TON_{Re} values of over 2100, representing the first application of the $^3\text{ILCT}$ state of a Re(I) carbonyl complex in a stable photocatalytic system.

INTRODUCTION

Rhenium(I) tricarbonyl complexes bearing polypyridine ligands are very popular and well-studied molecules, especially concerning their photochemistry and photophysics. These complexes have found many applications, especially in solar energy conversion, where their use for photoelectrochemical CO₂ reduction^{1–6} and as photosensitisers for hydrogen production are the most prominent ones.^{7–18} The *fac*-{Re(CO)₃}⁺ moiety makes these complexes excellent IR absorbers. The high sensitivity of the CO stretching modes to the electronic density around the metal centre, their very high IR absorption coefficients and the overall stability of this organometallic core allowed Re(I) tricarbonyl complexes to become one of the most studied systems by transient IR spectroscopy, and can be considered the closest analogues of [Ru(bpy)₃]²⁺ in terms of their widespread use as photosensitisers.^{19,20}

Re(I)-tricarbonyl diimine complexes typically exhibit a purely metal-to-ligand charge transfer (MLCT) or mixed ligand-to-ligand charge transfer (LLCT) absorption band centred around 380 nm, and the corresponding ligand-centred excitation bands at higher energies.²¹ Consequently, these dyes absorb almost exclusively ultraviolet or blue light, which has prompted the design, synthesis and study of complexes with enhanced absorption at lower energies. Most efforts in this direction have focused on the introduction of electron-withdrawing groups or the increase of the conjugation of the diimine ligand framework (Fig. 1A); in these cases, the absorption is red-shifted due to a stabilization of the ligand-centred π^* orbitals (typically the LUMO).²²

While the effects of substitution in the vicinity of the metal centre have been previously described for Re(I) tricarbonyl complexes,^{23–26} further understanding of the

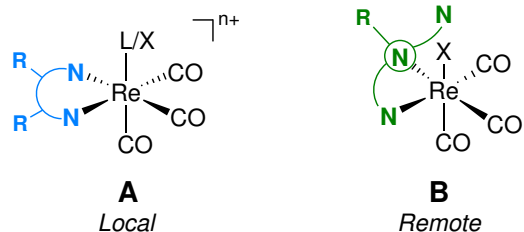
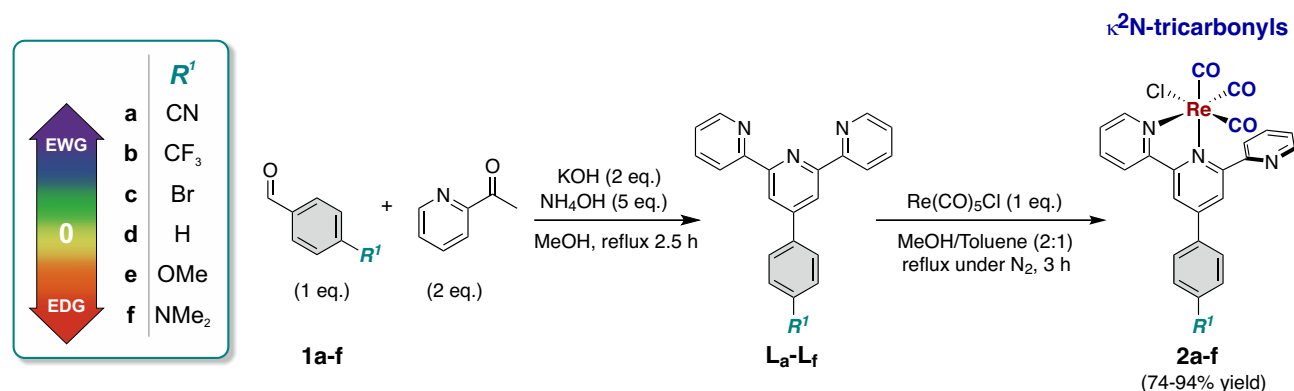


Figure 1. Different strategies for red-shifting the absorption of Re(I) carbonyl dyes: (A) by substituting the bipyridine ligands (stabilising the ligand π^* orbitals); (B) through remote substitution, affecting the HOMO and allowing for excited-state character switching.

effects of substitution far away from the metal centre (Fig. 1B) is needed, and constitutes a promising alternative to fine tune the properties of these complexes.

The photophysics and photochemistry of remote substituent effects in Re(I) complexes have been explored in the past by many groups. Amongst them, studies by Schanze and co-workers focused on remote substitution of the axial ligand in [Re(bpy)(CO)₃(L)]⁺-type complexes, where the L ligand was decorated with a dimethylamino group,²⁷ or a cation-responsive crown macrocycle.²⁸ This strategy was later combined with a dipyrrodo[3,2- α :2',3'-c]phenazine (dppz) ligand, replacing the bipyridine ligand,²⁹ and combined with a photoisomerisable stilbene-like moiety as shown by Perutz and co-workers.³⁰ The ultrafast dynamics of intramolecular electron transfer in an azacrown-ether-decorated complex were reported by Perutz, Moore and co-workers,³¹ who used transient UV-Visible absorption. Similarly, porphyrin-appended Re(I) carbonyl complexes have been studied by ultrafast transient IR (TRIR) and transient



Scheme 1. Synthetic route and structures of the compounds studied in the present work.

UV-Vis absorption spectroscopy,^{32,33} and it was shown that photoexcitation of these complexes may lead to ligand dissociation.³⁴ In addition, the electron transfer dynamics of porphyrin-appended Re(I) carbonyl complexes have been studied in NiO surfaces.³⁵

Most of the examples mentioned until now focus on substitution of the axial ligand. In our approach, we use the 2,2':6',2''-terpyridine (terpy) to operate on the α -diimine ligand instead. The terpy framework represents an ideal structural backbone for modification by substitution. In particular, phenyl-substituted terpyridine ligands have shown remarkable photophysical and photochemical properties by themselves,³⁶ as well as their complexes with Ru(II),^{37,38} Pt(II),³⁹ Zn(II),⁴⁰ Ir(III),⁴¹ and other transition metals. In most of these cases, the terpyridine ligand acts as a tridentate ligand, adopting a meridional configuration around the metal centre. In contrast, *fac*-Re(I) tricarbonyl complexes with terpyridine ligands contain a bidentate (κ^2N) terpyridine ligand in a bipyridine-like coordination fashion.^{20,42–44}

The photophysical properties of a few Re-based terpyridine complexes,^{45,46} as well as those with structurally-related bidentate N \wedge N ligands have been previously studied.^{47,48} Some of these evidenced long-lived intraligand charge-transfer (ILCT) states.⁴⁸

Despite the abundant literature on terpyridine-based Re(I)-tricarbonyl complexes, an in-depth systematic exploration of the tuning of ground and excited-state properties is missing. Moreover, the effect of substituents in the character of the lowest excited states has been only discussed in brief. In this regard, a recent report by Shillito, Gordon and co-workers showed how the switching in character of the lowest excited states (from MLCT to ILCT) frustrates the tuning of properties in Re(I) and Pt(II) complexes bearing triphenylamine-substituted 1,10-phenanthroline ligands.⁴⁹

In the present work, we focus on the effects of remote substitution across the 4'-(4-*R*¹-phenyl)-2,2':6',2''-terpyridine (terpy) framework in the photophysical and photochemical properties of Re(I) tricarbonyl complexes. We show that, in a complementary manner as has been described before, the introduction of electron-donating

substituents changes the localisation of the HOMO (instead of tuning the LUMO as shown in Ref. 23), leading to a change in the character of the lowest excited state from MLCT to intraligand charge-transfer (ILCT).

We report on the synthesis, spectroscopic, crystallographic and electrochemical characterisation of a series of Re(I) κ^2N -tricarbonyl (**2a-f**) complexes with substituted 4'-(4-*R*¹-phenyl)-2,2':6',2''-terpyridine ligands (**L_a-L_f**). Studying a series of complexes bearing substituents of different electron-donating abilities (from CN to NMe₂, Scheme 1) allowed us to correlate the observed properties with the electronic density on the terpyridine ligand. The ground and excited-state properties of these complexes were studied by UV pump-IR probe (in the fs to μ s range), electrochemistry, FT-IR spectroelectrochemistry (IR-SEC) and photoluminescence measurements. In addition, through a combined experimental and computational approach, we could establish the key differences between the characters of the lowest-lying excited states. Finally, we evaluated the potential utility of these complexes for photochemical energy conversion with proof-of-principle measurements of photocatalytic hydrogen evolution. To the best of our knowledge, this demonstrates for the first time the application of productive ³ILCT states of Re(I) carbonyl complexes in photocatalysis.

RESULTS AND DISCUSSION

Synthesis and characterization

The 4'-(4-*R*¹-phenyl)-2,2':6',2''-terpyridine ligands (**L_a-L_f**) were readily obtained in one step from 2-acetylpyridine and the corresponding 4-*R*¹-benzaldehyde using a modified Kröhnke methodology, as reported previously.^{50,51} This ligand framework and synthetic methodology enable easy modification at the 4' position of the terpyridine (tpy) ligand. The κ^2N -tricarbonyl complexes (**2a-f**) were obtained in excellent yields from Re^I(CO)₅Cl as air-stable yellow solids (**2f** as a yellow-green solid) by refluxing in MeOH/Toluene mixtures (See SI for details). Single crystal X-ray diffraction

analysis were performed for the κ^2N -tricarbonyl complexes **2a**, **2b**, and **2e**. Figure 2 shows the displacement ellipsoid plot of the structure of **2a** as a representative example.

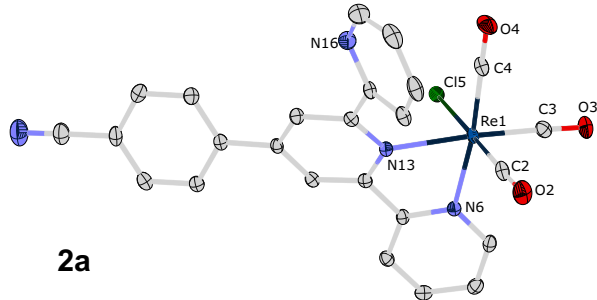


Figure 2. Displacement ellipsoid representation at the 50% probability level of the crystal structure of complex **2a**. Hydrogen atoms and solvent molecules omitted for clarity.

The structures of the κ^2N -tricarbonyl complexes show a bipyridine-like coordination of the terpyridine ligand to the $fac\text{-}\{\text{Re}(\text{CO})_3\}^+$ core, the two rings being twisted by about 10° . The third pyridine ring is rotated by ca. $45\text{--}50^\circ$, and the 4'-phenyl ring is rotated by $15\text{--}25^\circ$ with respect to the plane of the central pyridine ring. A brief discussion of the crystal structures, and a table of crystallographic parameters are given in the SI (Table S1). In the solution ^1H -NMR spectra of complexes (**2a-f**), we observe two sets of signals for the peripheral pyridine rings, supporting the κ^2N coordination with a dangling pyridine observed in the solid state.

Steady-State Spectroscopic Properties

The UV-Vis and FT-IR spectra of **2d-f** in DMF (as representative examples) are shown in Figure 3 (other spectra are provided in the SI, Figs. S1-S2 and Table S2). In the UV-Vis absorption spectra of the κ^2N -tricarbonyl complexes (**2a-f**) we observe a band centred around 380 nm with an extinction coefficient $\varepsilon \approx 4000 \text{ cm}^{-1} \text{ M}^{-1}$, typical of an MLCT band in Re(I) complexes.²¹ The higher energy bands are attributed to ligand-centred $\pi\text{-}\pi^*$ transitions. Time-dependent density functional theory (TD-DFT) calculations performed in Gaussian 09 rev. D.01⁵² nicely reproduce all these features (Fig. S3 in the SI).

The MLCT absorption band shows a hypsochromic shift of ca. 720 cm^{-1} as the electron donating character of the substituent increases from CN to OMe (values provided in Table S2 in the SI). These shifts are much smaller than those obtained upon direct substitution at the 4 and 4' positions of the bpy ligand (of ca. 6250 cm^{-1} between NO_2 and NH_2),^{23,53} and suggest a small, albeit observable electronic effect of substitution in the 4'-phenyl ring of the terpy ligands when going from CN to OMe. While the spectra of the complexes with electron-withdrawing substituents do not show significant changes, complexes

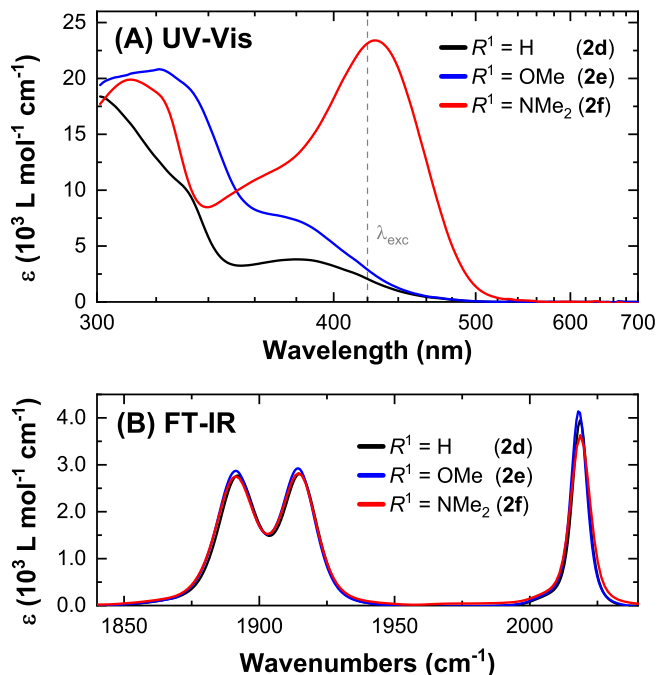


Figure 3. (A) UV-Vis and (B) FT-IR spectra of **2d-f** in DMF, as representative examples. The dashed line in **A** indicates the excitation wavelength used in the transient absorption experiments (420 nm).

with more electron-donating groups show distinct features in their UV-Vis spectra. For **2e** ($R^1 = \text{OMe}$) we observe a new shoulder at lower energies, which evolves into a very intense absorption band in **2f**, bearing the more electron-donating $R^1 = \text{NMe}_2$ moiety. This additional, low energy band (Figure 3, red), has a significantly higher extinction coefficient than typical MLCT or even ligand-centred $\pi\text{-}\pi^*$ transitions, providing a first hint into its different character.

In the FT-IR absorption spectra of **2a-f** in DMF, we observe the typical features of the $fac\text{-}\{\text{Re}(\text{CO})_3\}^+$ moiety: three strong ν_{CO} bands at ca. 2019, 1915 and 1892 cm^{-1} , corresponding to modes of $A'(1)$, A'' and $A'(2)$ symmetries, respectively. The ν_{CO} frequencies shift only $2\text{--}4 \text{ cm}^{-1}$ (Table S2 in the SI), contrasting the higher shifts observed upon direct substitution at the bpy ligand (in the order of $5\text{--}20 \text{ cm}^{-1}$),²³ and can be explained by the remote character of substitution in these complexes.

Characters of the Lowest Excited States

We now turn to (TD-)DFT calculations to understand the effects of the substituents in the electronic structure of these complexes. We observe an increase in the relative energies of the HOMO and LUMO orbitals with more donating groups, the energies of the latter having a more pronounced dependence (Figure S4 in the SI).

While the location of the LUMO remains largely unaltered throughout the series, we observe that

as the electron-donating character of the substituent is increased, the HOMO gradually shifts from the $\{\text{Re}(\text{CO})_3\}^+$ moiety towards the 4'-phenyl moiety of the terpy ligand (Figure 4), until it is localised entirely on the latter, for $R^1 = \text{NMe}_2$.

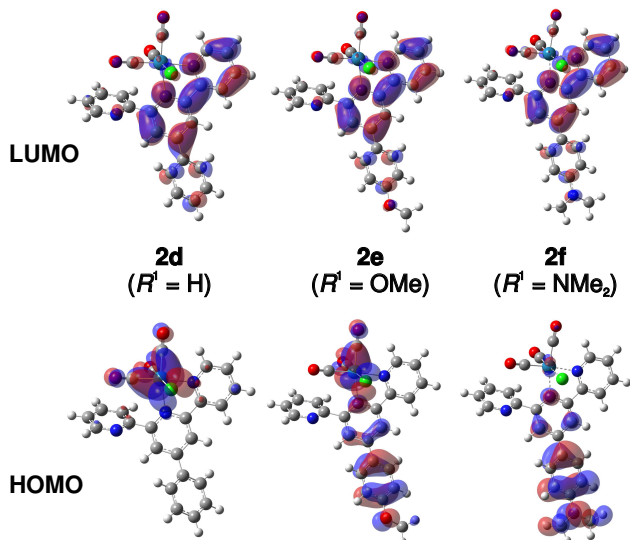


Figure 4. Calculated HOMO and LUMO orbitals of **2d**, **2e** and **2f**. Orbitals shown at $|\phi| = 0.025$ a.u.

These observations are supported by the charge density difference (CDD) isosurfaces calculated for the $S_1 \leftarrow S_0$ transition, shown in Figure 5 for the unsubstituted, OMe and NMe_2 -substituted complexes (**2d**, **2e**, and **2f**, respectively). The CDD isosurfaces were calculated using MultiWfn v3.5.⁵⁴

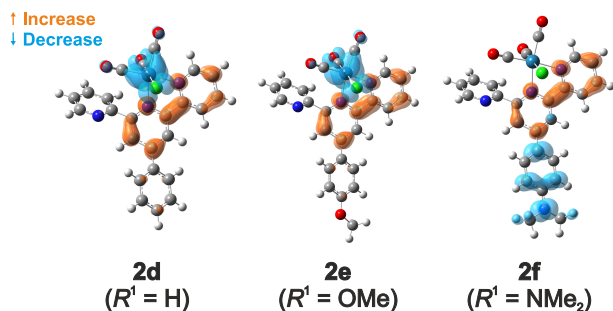


Figure 5. Charge density difference (CDD) isosurfaces of the $S_1 \leftarrow S_0$ transition of **2d-f**, shown at $|\Delta\rho| = 0.002$ a.u.

For complex **2d** (and those with more electron withdrawing substituents) it is clear that this transition has the expected MLCT character. Surprisingly, the despite the change in the localisation of the HOMO observed for complex **2e**, the $S_1 \leftarrow S_0$ transition conserves an MLCT character (further supported by transient IR data, discussed next). In contrast, the $S_1 \leftarrow S_0$ transition in the NMe_2 -substituted complex has a strong ILCT character—with the NMe_2 group acting as the donor, and

the metal-coordinated κ^2N -terpy as the acceptor.

Excited-state dynamics

To understand the excited-state dynamics of these complexes, we performed transient absorption experiments with UV pump and ultrashort broadband mid-IR pulses derived from a home-built OPA as the probe (complete experimental details are given in Section 1.3 of the SI).^{55–57}

Transient IR spectra of the complexes **2a-e** in air-saturated DMF, recorded upon excitation with 420 nm ultrashort pulses show the typical features of the excited $^3\text{MLCT}$ state of $\text{Re}(\text{I})$ tricarbonyl dyes within 500 fs of excitation. The TRIR spectra of **2d** as a representative example is shown in Figure 6. These bands show a time-dependent blue shift, on a timescale of ca. 5 ps, attributed to a convolution of ultrafast intersystem crossing (ISC, within ~ 100 fs) and vibrational relaxation on the excited state, in agreement with previous reports.^{10,48,58}

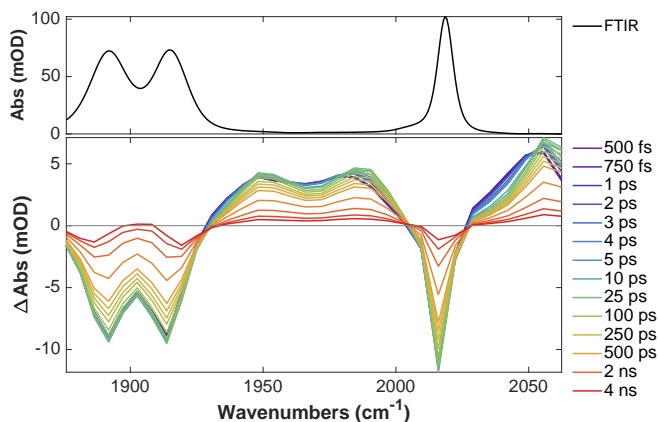


Figure 6. FT-IR spectrum (*top*) and magic-angle UV pump-IR probe transient spectra (*bottom*) of **2d** (5 mM in DMF) at different pump-probe delays.

For complex **2f**, the situation is different: transient IR spectroscopy yielded the definitive experimental evidence for a $^3\text{ILCT}$ state in this complex. Immediately after excitation, we observed in the TRIR spectra of **2f** in DMF (Figure 7) two sets of ESA bands in the ν_{CO} region: a single, clearly resolved band around 1994 cm^{-1} , and a set of two unresolved bands in the 1860 cm^{-1} region, which partially overlap with the ground-state bleaches.

The red shifts of the ESA bands suggest an increase of electron density around the $\text{Re}(\text{I})$ centre upon photoexcitation, closely resembling the difference spectra of the singly reduced species (Fig. 7, *purple dotted line*) observed by IR spectroelectrochemical studies (IR-SEC). These features are very well reproduced by DFT calculations of the lowest triplet excited state and the singly reduced NMe_2 -substituted complex (Fig. S5 in the SI). After the initial blue shift of the bands in a 5 ps timescale, the observed signal remained constant for more than 4 ns,

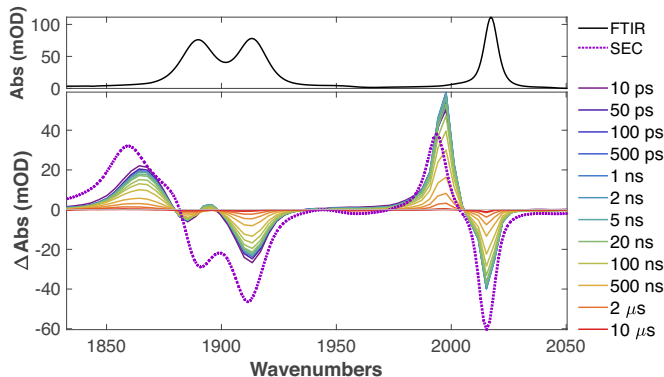


Figure 7. FT-IR spectrum (*top*) and UV pump-IR probe transient spectra (*bottom*) of **2f** (5 mM in N_2 -purged DMF) at different delays (ps- μ s timescales). The IR-SEC difference spectrum at -1.8 V vs Fc^+/Fc (first reduction) is overlaid with the pump-probe spectra (purple dotted line, $\Delta Abs \times 0.4$).

(see Fig. S6 in the SI). To observe the decay of these features (and hence extract the actual excited-state lifetimes), we performed a second set of TRIR measurements comprising timescales from 10 ps to over 10 μ s, using a setup based on two synchronised amplifiers.⁵⁹ From these measurements, we obtained a lifetime of 380 ± 20 ns in a nitrogen-purged DMF solution for **2f**. The significantly longer lifetime of this complex (ca. 260 times longer than that of **2d**) can be explained by the different characters of the lowest triplet excited states.

These observations contrast with the TRIR data of complexes **2a-e** (Figure 6). In those cases, excitation of the MLCT band *decreases* the electronic density around the metal centre (evidenced by blue-shifted ESA bands), and the transient signals decay significantly faster.

On the ps- μ s setup, and under the same measurement conditions, we obtained a lifetime of 2.3 ± 0.2 ns for **2e** ($R^1 = OMe$) in nitrogen-purged DMF, which agrees quantitatively with the lifetime obtained in the ultrafast experiments in air-saturated DMF solutions. This illustrates the negligible effects of oxygen on the lifetimes of all other complexes, showing also the consistency of the kinetics obtained from the different setups.

The photophysical properties of ILCT states of Re(I) tricarbonyls have been previously studied in complexes bearing 3-substituted-1-(2-pyridyl)-imidazo[1,5- α]pyridine ligands.⁴⁸ The ILCT character of these complexes was largely independent from the substituents (ranging from NO_2 to NMe_2), in sharp contrast with our observation for the Re(I) complexes with 4'-(4- R^1 -phenyl)-2,2':6',2''-terpyridine ligands. In our case, only the NMe_2 -substituted complex (**2f**) shows a significant ILCT, displaying similar characteristic TRIR signatures, but a significantly longer excited-state lifetime.

A complementary approach, based on tuning the axial ligand, has also shown that 3ILCT lifetimes can be modulated from 27 ns to 6 μ s when the axial ligand is changed from pyridine to bromide. This opens additional pathways for future modifications of the complexes studied

in this work, and highlights the interplay between close-lying MLCT and long-lived ILCT states. In their work Gordon and co-workers show that the change in emission lifetimes does not arise from switching of molecular orbitals (as in our case, where the HOMO shifts with the substituent), close-lying deactivating states, contributions from a halide-to-ligand charge transfer state (XLCT) or changes in spin-orbit coupling.⁶⁰

In our case, we observe a systematic change in the 3MLCT lifetimes and reduction potentials (Figure 8 and Fig. S7 in the SI). The lifetimes increase from 0.58 to 2.3 ns between the CN and OMe-substituted complexes, while the reduction potentials become more negative, shifting from -1.6 to -1.8 V vs Fc^+/Fc (discussed next). The fitted lifetimes of all complexes can be found on Table S2 in the SI.

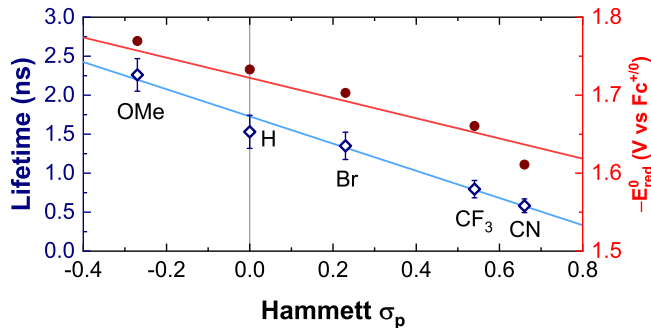


Figure 8. Linear correlations between the 3MLCT lifetimes (from transient IR, in blue), the observed ground-state reduction potentials (in red), and the Hammett σ_p substituent constants for complexes **2a-e**. Complex **2f** deviates significantly from the linearity of the lifetime plot, and is excluded for clarity.

The frequency shift of -17 cm^{-1} observed for the $a'(1)$ band in the TRIR spectra of **2f** in DMF is similar to the ca. -20 cm^{-1} shift reported for complexes with 3-substituted-1-(2-pyridyl)-imidazo[1,5- α]pyridine ligands (possessing also an ILCT excited state),⁴⁸ and is similar to the ca. -24 cm^{-1} shift observed upon electron transfer from the porphyrin to the rhenium moiety in the porphyrin-appended Re(I) tricarbonyl complexes studied by Perutz and co-workers.³² The latter, however, is in better agreement with the -24 cm^{-1} shift observed for the singly reduced **2f**⁻, obtained by spectroelectrochemistry (see below). Overall, these numbers illustrate the small but significant difference between a *formally* reduced complex, and an *apparent* reduced environment around the *fac*- $\{Re(CO)_3\}^+$ moiety arising from intramolecular charge transfer.

Photochemical and Redox Properties

To better understand the excited-state properties and to estimate the applicability of these complexes as photosensitisers, we evaluated the excited-state redox

potentials, which were estimated according to equations 1 and 2:

$$E_{\text{red}}^{\circ'}(^3[\text{Re}^{\text{I}}]^*) = E_{\text{red}}^{\circ'} + \Delta G_{\text{ST}} \quad (1)$$

$$E_{\text{ox}}^{\circ'}(^3[\text{Re}^{\text{I}}]^*) = E_{\text{ox}}^{\circ'} - \Delta G_{\text{ST}} \quad (2)$$

where $E_{\text{red}}^{\circ'}$ and $E_{\text{ox}}^{\circ'}$ are the ground-state reduction and oxidation potentials, respectively, and ΔG_{ST} is the singlet-triplet energy gap.

The ground-state redox properties of these complexes were studied by cyclic voltammetry (CV) in 0.1 M $[\text{Bu}_4\text{N}][\text{PF}_6]$ in DMF at room temperature. The cyclic voltammograms of selected complexes are shown in Figure 9. All complexes show a partially irreversible two-electron reduction ($E_{\text{red}}^{\circ'}$), taking place at ca. -1.7 V vs Fc^+/Fc . The oxidation was outside of the electrochemical window of our experiment ($E_{\text{ox}}^{\circ'} > 0.5$ V vs Fc^+/Fc).

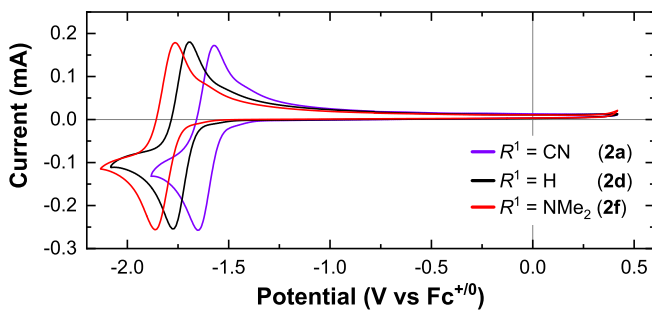


Figure 9. Cyclic voltammograms of selected complexes in 0.1 M $[\text{Bu}_4\text{N}][\text{PF}_6]$ in DMF. Scan rate: 100 mV s^{-1} .

From this, we observe that $E_{\text{red}}^{\circ'}$ becomes more negative with more electron-donating substituents (Table I), showing an excellent linear correlation with the Hammett σ_p substituent constants (Figure 8). This demonstrates that tunability in a range of ± 200 mV can be achieved without significantly altering the optical properties of these complexes (for **2a-e**), a desirable feature for fine-tuning the energetics of ground- and excited-state electron transfer processes involving these complexes.

At the same time, we note that the long-lived ILCT state achieved in the NMe_2 -substituted complex has still comparable excited-state reduction potentials (only ca. 200 mV below those of the rest of the complexes in the series), while absorbing light with comparable extinction coefficients over 100 nm further to the red.

Emission spectra of all complexes were measured in DMF at room temperature and at 77 K in a 2-methyltetrahydrofuran (2-MeTHF) glass (Figure S8 in the SI). The ΔG_{ST} values were obtained from a linear fit of the high energy side of the low-temperature emission spectra, as described previously (Figure S9 in the SI).²² These values also show a very good correlation with the Hammett σ_p substituent constants (except for **2f**), and illustrate that more electron-donating substituents can increase ΔG_{ST} up to a certain limit, before any further increase in the electronic density results in a decrease of ΔG_{ST} instead.

TABLE I. Ground- and excited-state redox properties of the studied complexes in DMF

R^1	$E_{\text{red}}^{\circ'}$ (V) ^a	$\Delta G_{\text{ST}}^{(\text{exp})}$ (eV) ^b	$\Delta G_{\text{ST}}^{(\text{theo})}$ (eV) ^c	$(E_{\text{red}}^{\circ'})^*$ (V) ^d
2a) CN	-1.61	2.42	2.38	0.80
2b) CF_3	-1.66	2.46	2.44	0.79
2c) Br	-1.70	2.46	2.46	0.76
2d) H	-1.73	2.48	2.49	0.75
2e) OMe	-1.77	2.50	2.47	0.73
2f) NMe_2	-1.81	2.37	2.06	0.56

^a Electrochemical potential in V vs. Fc^+/Fc in DMF.

^b From a linear fit of the high-energy side of the 77 K emission spectrum in 2-MeTHF.

^c Energy difference between the optimised ground and lowest triplet excited state structures.

^d Excited-state potentials calculated from eq. 1.

At room temperature, all complexes exhibit a moderately intense, broad and unstructured emission (very strong in the case of the NMe_2 complex, **2f**). The position of the emission maxima correlate well with the Hammett σ_p substituent constants, showing a blue shift with more electron-donating groups. At cryogenic temperatures (77 K), the emission spectra complexes **2a-e** show a significant hypsochromic shift, characteristic of emission from a $^3\text{MLCT}$ state. Complex **2f**, in contrast, deviates significantly from this behaviour. The emission of **2f** shows instead a bathochromic shift upon cooling, and the appearance of vibronic structure, suggestive of emission from a ligand-localised triplet state.⁶¹ These observations suggest that the character of the lowest triplet excited state of the NMe_2 -substituted complex changes upon cooling. At room temperature, it has a significant intraligand charge transfer (ILCT) character, also supported by results discussed in the previous section.

The DFT-calculated ΔG_{ST} values for the $\kappa^2\text{N}$ complexes were in excellent agreement with those found in the experiment, with a mean deviation of ± 0.02 eV for all complexes (except **2f**, which deviated by -0.3 eV). The ground- and excited-state redox properties are summarised in Table I.

To identify the spectral signatures of the redox species observed in the cyclic voltammetry experiments, we performed IR spectroelectrochemical (IR-SEC) studies in 0.1 M $[\text{Bu}_4\text{N}][\text{PF}_6]$ in DMF. The IR-SEC spectra of **2d** are shown in Fig. 10 as a representative example.

The two-electron reduction process could be resolved in the IR-SEC experiments into two overlapping and consecutive single-electron reductions, evidenced by significant incremental red shifts of the ν_{CO} bands (Fig. 10).

Further evidence for the two-electron nature of this reduction comes from the ca. 96 mV peak-to-peak separation (at a scan rate of 100 mV s^{-1}), and the small shoulder observed at less negative potentials (Fig. 9). In all cases, an excellent agreement was found between

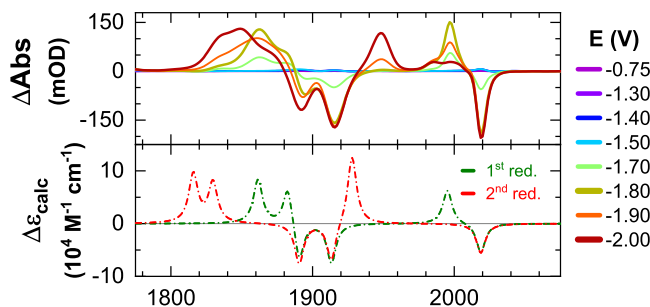


Figure 10. Experimental (solid lines) and calculated (dashed lines) difference IR spectra of the redox states of **2d**. Experimental spectra measured in 0.1 M [Bu₄N][PF₆] in DMF. Potentials vs Fc⁺/Fc. Theoretical frequencies were scaled by 0.97 to better match the experimentally obtained values.

the calculated and experimental difference spectra of the corresponding redox states. The partial irreversibility of the second reduction process is attributed in both cases to loss of the chloride ligands (also reproduced in the DFT calculations, where optimisation of the doubly reduced species led to Cl dissociation), agreeing with previous reports of related complexes.⁶²

Photocatalytic hydrogen evolution experiments

Considering the excited-state redox potentials and lifetimes exhibited by these complexes, we performed a series of homogeneous proof-of-principle photocatalysis experiments in DMF. To focus only on the H₂ evolution half-reaction, triethanolamine (TEOA, 1 M) was used as a sacrificial electron donor and triflic acid (TfOH, 0.1 M) as the proton source. For these test experiments, we chose [Co(dmgh₂)₂]²⁺ (0.5 mM) as a catalyst, which was prepared *in situ* from Co(BF₄)₂·6 H₂O and excess dmgh₂. As representative examples, we tested complexes **2d** and **2f**, as well as [Re(bpy)(CO)₃(NCS)] (**RePS**) under the same conditions (with [Re]=0.5 mM and λ_{exc} = 390 nm). The latter complex was used to benchmark the performance of our complexes in comparison to a well-studied system.^{63,64}

Under these conditions, we observed significant and prolonged hydrogen evolution only for **2d** (Figure S10 in the SI), yielding final turnover numbers for the photosensitiser (TON) of 580±40 over 7 days. We observed a bimodal decay of the turnover frequency (TOF), and a significant decrease in the rate after 4.5 days. These results suggest that the integrity of the catalyst represents the limiting factor for the long-term stability of this photocatalytic system, as discussed in previous reports of related systems.⁶⁵ We did not observe hydrogen evolution using complex **2f** at these high concentrations, which we attribute to accumulation of the reduced photosensitiser and subsequent degradation.⁶⁴

Considering this last result, and the very long lifetime of complex **2f** and its intense absorption extending un-

til ca. 500 nm, we performed additional photocatalytic experiments (Figure 11) with λ_{exc} = 453 nm and higher dmgh₂ concentrations (3.5 mM), while using a tenfold lower photosensitiser concentration ([**2f**] = 50 μM). All other parameters were kept constant.

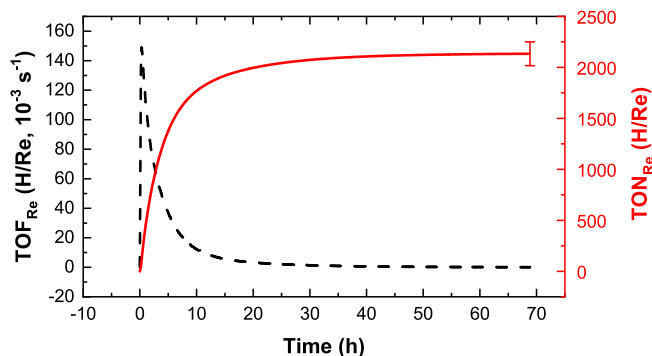


Figure 11. Hydrogen evolution from **2f** as a photosensitiser. Conditions: [**2f**] = 50 μM, [Co] = 0.5 mM, [dmgh₂] = 3.5 mM, 1 M TEOA, 0.1 M TfOH in DMF, λ_{exc} = 453 nm.

The very high turnover numbers (2130±120) and hydrogen production rates (up to ca. 40 nmol s⁻¹) obtained under these conditions compare very favourably with those obtained for a closely related system using [Re(bpy)(CO)₃(NCS)] as photosensitiser.^{63,64} While strict comparisons of the TOF and TON values are inadequate, it is worth mentioning that under these conditions, complex **2f** is a remarkably stable photosensitiser. The results shown in this work constitute, to the best of our knowledge, the first example of a system where the long-lived ³ILCT state of a Re(I) complex is used for photocatalytic hydrogen production, being involved in multielectron transfer steps in an efficient manner. We believe that the long-term stability of this system might be improved by fine-tuning the conditions of the photocatalytic experiments, which are outside the scope of the present work.

To gain a deeper understanding of the initial photochemical steps in the photocatalytic cycle, and in particular, to evaluate the potential differences between ILCT and MLCT excited-state reactivity, we performed emission quenching, as well as TRIR experiments in the ps-μs timescales of complexes **2d** and **2f** in presence of TEOA. For **2d**, we observed a very small change in the excited-state kinetics and emission intensities, leading to a diffusion-limited quenching rate $k_Q \approx 4 \times 10^8 \text{ M}^{-1} \text{ s}^{-1}$. We find this number of qualitative character, given the very short lifetime of **2d**, which limits the possibility of studying the intermolecular electron transfer steps in this complex.

Complex **2f**, in contrast, presented an unexpected behaviour. Upon addition of TEOA, we observed the appearance of a strongly emissive blue-shifted band, whose intensity increased with increasing concentrations of TEOA. The absorption spectra remained unchanged. At the same time, the spectral features and kinetics of

2f (1 mM in degassed DMF) remained largely unchanged in a concentration range from 1 mM to 1 M TEOA (containing 10 mol% TfOH), hinting at a different order of events in the photocatalytic cycle of **2f**. Transient IR spectra recorded in absence of TfOH also did not show any difference with respect to those of pure **2f** in DMF.

In the 'conventional' photocycle, the $^3\text{MLCT}$ excited state of a Re(I) complex (like **RePS**) is reductively quenched in a bimolecular fashion by TEOA, and it is this reduced species which transfers the electrons to the proton reduction catalyst.^{14,64} If the $^3\text{ILCT}$ excited state of **2f** is not quenched by TEOA—and given the fact that the system *does* evolve significant amounts of hydrogen—we hypothesise that this complex transfers the electron directly to the cobalt catalyst (considering its very long lifetime). After this electron transfer, the oxidised **2f**⁺ is regenerated by TEOA at longer timescales.

To prove this hypothesis, we performed TRIR experiments of **2f** with different concentrations of $[\text{Co}(\text{dmgH})_2]^{2+}$ ranging from 10 to 75 mM (the cobalt complex was prepared as a stock solution from anhydrous CoBr_2 and 3 eq. dmgH_2 in DMF). From a Stern–Volmer analysis of the TRIR kinetic data (Figure S11 in the SI), we obtained a second-order quenching rate constant of $k_{\text{Co}} = (2.0 \pm 0.2) \times 10^8 \text{ M}^{-1} \text{ s}^{-1}$ for electron transfer between **2f** and $[\text{Co}(\text{dmgH})_2]^{2+}$. This value of k_{Co} compares very well with the reported values of 1.3×10^8 and $2.5 \times 10^8 \text{ M}^{-1} \text{ s}^{-1}$ for electron transfer between reduced **RePS**[−] or $[\text{Re}(\text{bpy})(\text{CO})_3\text{Br}]^−$, respectively, and $[\text{Co}(\text{dmgH})_2]^{2+}$. This rate is also significantly slower than the $1.23 \times 10^9 \text{ M}^{-1} \text{ s}^{-1}$ quenching rate between photoexcited **RePS**^{*} and $[\text{Co}(\text{dmgH})_2]^{2+}$, thus excluding this mechanism.⁶⁴

The absence of new transient features and long-lived signals in the TRIR spectra of **2f** with $[\text{Co}(\text{dmgH})_2]^{2+}$ (independent of the presence of TEOA) may suggest that either (i) there is a fast back electron transfer from the cobalt complex in absence of TEOA; or (ii) fast electron transfer from TEOA (present in a large excess) to **2f**⁺ takes place after the initial quenching event in the three component system.

Combining the insights gained from these experiments, we believe that the formation of an exciplex between excited **2f**^{*} and TEOA can simultaneously explain the changes in the emission spectra and the unchanged TRIR data. The formation of a metal complex–molecule exciplex has been observed before,⁶⁶ with the case of $[\text{Re}(4,7\text{-diphenyl-1,10-phenanthroline})(\text{CO})_3\text{Cl}]$ and N,N-dimethylaniline (DMA) in decaline being particularly relevant in the context of our work. In this system, even very low concentrations ($\sim 10^{-3} \text{ M}$) of DMA were enough to observe a new, red-shifted emission band.⁶⁷ While our specific scenario is different—namely a more polar solvent and a different quencher—complex **2f** has a very large charge transfer character upon photoexcitation (as shown in Fig. 5), leading to a large change in dipole moment, which would render formation of a charge transfer exciplex with TEOA feasible.

Additional mechanistic studies of these complexes with the purpose of unravelling the nature of this process and its solvent dependence will reveal further differences in the reactivity and photophysical properties of the $^3\text{ILCT}$ vs $^3\text{MLCT}$ excited states, easily switched in these complexes by a remote substitution in the ligand framework.

CONCLUDING REMARKS

The ground and excited states of a series of rhenium(I) tricarbonyl complexes with substituted 4'-(4-*R*¹-phenyl)-2,2':6',2''-terpyridine ligands were analysed by steady-state and time-resolved spectroscopic methods. We found excellent correlations between the evaluated spectroscopic and electrochemical properties of these complexes and the Hammett σ_p substituent constants, showing their tunability even by changing the substituent in a remote position of the ligand framework. Cyclic voltammetry and IR-SEC revealed an irreversible stepwise two-electron reduction, which in turn allowed us to assign the identities and spectral signatures of the one- and two-electron reduced species.

The NMe₂-substituted complex (**2f**) showed notably exceptional lifetime and spectroscopic properties compared to other complexes of the same series. In this complex, the lowest singlet and triplet excited states have both an ILCT character, demonstrated by transient IR and emission spectra, and supported by detailed (TD-)DFT calculations. The particularly long triplet lifetime of ca. 380 ns obtained for the NMe₂-substituted complex (vs. ca. 1.5 ns for the unsubstituted complex) suggests that very strongly donating groups can lead to distinct photophysical and photochemical properties, and opens new avenues to explore further substituent-related modifications to the terpyridine ligand framework. We conclude that judicious ligand-based substitutions can still be exploited to access long-lived, strongly emissive, yet sufficiently reducing excited states of complexes with significantly red-shifted absorption, which would perform as better photosensitisers by using a wider portion of the solar spectrum. In this regard, our approach to enhance light absorption through remote substitution is complementary to those that have been explored so far, and benefits from the simplicity and scalability of the synthesis of the substituted terpyridine ligands.

In proof-of-principle homogeneous photocatalytic experiments, we demonstrated stable H₂ evolution over a period of 7 days with complex **2d**, and a fast and sustained H₂ evolution from complex **2f** in a photocatalytic system with tenfold smaller photosensitiser concentrations, reaching turnover numbers over 2100 using standard $[\text{Co}(\text{dmgH})_2]^{2+}$ as a catalyst. Using transient IR spectroscopy, we tentatively assign direct electron transfer from **2f**^{*} to the proton reduction catalyst, instead of reductive quenching by the sacrificial donor (TEOA). Changes in the emission spectra of **2f** Further mechanistic studies are needed to explain this in detail, focus-

ing on the differences in reactivity between complexes operating from a $^3\text{ILCT}$ vs $^3\text{MLCT}$ excited state. The application of **2f** for photocatalytic hydrogen evolution constitutes, to the best of our knowledge, the first example of the use of long-lived $^3\text{ILCT}$ states in Re(I) tricarbonyl complexes for photocatalytic hydrogen production, and shows the potential of the terpyridine framework for further modifications and mechanistic studies of the rich photochemistry of these complexes.

ASSOCIATED CONTENT

Supporting Information

Full experimental details, including synthetic procedures, characterization details, crystallographic discussions, details about the transient absorption and electrochemistry experiments; UV-Vis absorption, emission, NMR and FT-IR spectra of all complexes; IR spectroelectrochemical data; details of the computational calculations, and additional tables and figures (PDF). This material is available free of charge via the Internet at <http://pubs.acs.org>.

Accession codes

CCDC entries 2012297 (**2a**), 2012296 (**2b**) and 2012298 (**2e**) contain the supplementary crystallographic data for this paper. These can be obtained free of charge via the Internet at <http://www.ccdc.cam.ac.uk/structures/>, or by contacting the Cambridge Crystallographic Data Centre, 12 Union Road, Cambridge CB2 1EZ, UK.

AUTHOR INFORMATION

Corresponding Author

* E-mail: Ricardo.Fernandez@chem.uzh.ch;
Phone: +41 44 635 44 73; Fax: +41 44 635 68 38

ORCID identifiers

Ricardo Fernández-Terán 0000-0002-4665-3520
Laurent Sévery 0000-0002-6546-379X

Funding Sources

This research was funded through the Swiss National Science Foundation (Sinergia Project CRSII2 160801/1, and AP Energy Grant PYAPP2 160586), and the University Research Priority Program (URPP) for Solar Light into Chemical Energy Conversion (LightChEC) of the University of Zurich.

Notes

The authors declare no competing financial interest.

ACKNOWLEDGMENTS

We thank Prof. Dr. Peter Hamm and Prof. Dr. S. David Tilley for their valuable input and encouragement. We thank Prof. Dr. Roger Alberto and his group for allowing us to use the photochemical H_2 evolution detection system and laboratory infrastructure. Dr. Benjamin Probst-Rüd is greatly acknowledged for his valuable support in the photocatalytic H_2 evolution experiments, and insightful discussions. Prof. Dr. Bernhard Spingler is acknowledged for helpful crystallographic discussions. We also thank Dr. Jan Helbing and Gökçen Tek for insightful discussions; and Olga Božović for proofreading the manuscript and providing helpful comments.

REFERENCES

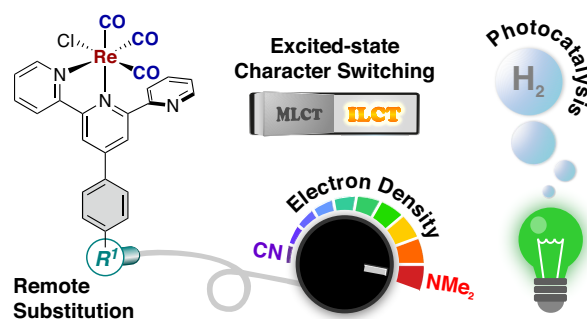
- (1) H. Takeda, K. Koike, H. Inoue, and O. Ishitani, Development of an efficient photocatalytic system for CO_2 reduction using rhenium(I) complexes based on mechanistic studies, *J. Am. Chem. Soc.* **130**, 2023 (2008).
- (2) H. Takeda and O. Ishitani, Development of efficient photocatalytic systems for CO_2 reduction using mononuclear and multinuclear metal complexes based on mechanistic studies, *Coord. Chem. Rev.* **254**, 346 (2010).
- (3) B. Kumar, M. Llorente, J. Froehlich, T. Dang, A. Sathrum, and C. P. Kubiak, Photochemical and Photoelectrochemical Reduction of CO_2 , *Annu. Rev. Phys. Chem.* **63**, 541 (2012).
- (4) T. Morimoto, T. Nakajima, S. Sawa, R. Nakanishi, D. Imori, and O. Ishitani, CO_2 capture by a rhenium(I) complex with the aid of triethanolamine, *J. Am. Chem. Soc.* **135**, 16825 (2013).
- (5) Y. Kou, Y. Nabetani, D. Masui, T. Shimada, S. Takagi, H. Tachibana, and H. Inoue, Direct detection of key reaction intermediates in photochemical CO_2 reduction sensitized by a rhenium bipyridine complex, *J. Am. Chem. Soc.* **136**, 6021 (2014).
- (6) M. Schreier, P. Gao, M. T. Mayer, J. Luo, T. Moehl, M. K. Nazeeruddin, S. D. Tilley, and M. Grätzel, Efficient and selective carbon dioxide reduction on low cost protected Cu_2O photocathodes using a molecular catalyst, *Energy Environ. Sci.* **8**, 855 (2015).
- (7) X. Yi, J. Zhao, J. Sun, S. Guo, and H. Zhang, Visible light-absorbing rhenium(I) tricarbonyl complexes as triplet photosensitizers in photooxidation and triplet-triplet annihilation upconversion, *J. Chem. Soc. Dalt. Trans.* **42**, 2062 (2013).
- (8) A. O. T. Patrocínio, K. P. Frin, and N. Y. Murakami Iha, Solid state molecular device based on a rhenium(I) polypyridyl complex immobilized on TiO_2 films, *Inorg. Chem.* **52**, 5889 (2013).
- (9) Y. Gao, S. Sun, and K. Han, Electronic structures and spectroscopic properties of rhenium (I) tricarbonyl photosensitizer: $[\text{Re}(4,4'-(\text{COOEt})_2-2,2'\text{-bpy})(\text{CO})_3\text{py}]\text{PF}_6$, *Spectrochim. Acta - Part A Mol. Biomol. Spectrosc.* **71**, 2016 (2009).
- (10) A. El Nahhas, C. Consani, A. M. Blanco-Rodríguez, K. M. Lancaster, O. Braem, A. Cannizzo, M. Towrie, I. P. Clark, S. Zálaiš, M. Chergui, and A. Vlček, Ultrafast excited-state dynamics of rhenium(I) photosensitizers

- [Re(Cl)(CO)₃(N,N)] and [Re(imidazole)(CO)₃(N,N)]⁺: Diimine effects, *Inorg. Chem.* **50**, 2932 (2011).
- (11) C. L. Anfuso, R. C. Snoeberger, A. M. Ricks, W. Liu, D. Xiao, V. S. Batista, and T. Lian, Covalent attachment of a rhenium bipyridyl CO₂ reduction catalyst to rutile TiO₂, *J. Am. Chem. Soc.* **133**, 6922 (2011).
 - (12) J. Liu and W. Jiang, Photoinduced hydrogen evolution in supramolecular devices with a rhenium photosensitizer linked to FeFe-hydrogenase model complexes, *Dalt. Trans.* **41**, 9700 (2012).
 - (13) M. Abdellah, A. M. El-Zohry, L. J. Antila, C. D. Windle, E. Reisner, and L. Hammarström, Time-resolved IR spectroscopy reveals a mechanism with TiO₂ as a reversible electron acceptor in a TiO₂–Re catalyst system for CO₂ photoreduction, *J. Am. Chem. Soc.* **139**, 1226 (2017).
 - (14) B. Probst, M. Guttentag, A. Rodenberg, P. Hamm, and R. Alberto, Photocatalytic H₂ production from water with rhenium and cobalt complexes, *Inorg. Chem.* **50**, 3404 (2011).
 - (15) M. Guttentag, A. Rodenberg, R. Kopelent, B. Probst, C. Buchwalder, M. Brandstätter, P. Hamm, and R. Alberto, Photocatalytic H₂ production with a rhenium/cobalt system in water under acidic conditions, *Eur. J. Inorg. Chem.* **2012**, 59 (2012).
 - (16) M. Guttentag, A. Rodenberg, C. Bachmann, A. Senn, P. Hamm, and R. Alberto, A highly stable polypyridyl-based cobalt catalyst for homo- and heterogeneous photocatalytic water reduction, *Dalt. Trans.* **42**, 334 (2013).
 - (17) A. Rodenberg, M. Oraziatti, B. Probst, C. Bachmann, R. Alberto, K. K. Baldrige, and P. Hamm, Mechanism of photocatalytic hydrogen generation by a polypyridyl-based cobalt catalyst in aqueous solution, *Inorg. Chem.* **54**, 646 (2015).
 - (18) A. Rodenberg, M. Oraziatti, M. Mosberger, C. Bachmann, B. Probst, R. Alberto, and P. Hamm, Quinones as Reversible Electron Relays in Artificial Photosynthesis, *ChemPhysChem* **17**, 1321 (2016).
 - (19) K. Kalyanasundaram, Photophysics, photochemistry and solar energy conversion with tris(bipyridyl)ruthenium(II) and its analogues, *Coord. Chem. Rev.* **46**, 159 (1982).
 - (20) A. Juris, S. Campagna, I. Bidd, J. M. Lehn, and R. Ziessel, Synthesis and photophysical and electrochemical properties of new halotricarbonyl(polypyridine)rhenium(I) complexes, *Inorg. Chem.* **27**, 4007 (1988).
 - (21) M. Wrighton and L. David, The Nature of the Lowest Excited State in Tricarbonylchloro-1,10-phenanthroline-rhenium(I) and Related Complexes, *J. Am. Chem. Soc.* **96**, 998 (1974).
 - (22) D. A. Kurtz, K. R. Brereton, K. P. Ruoff, H. M. Tang, G. A. Felton, A. J. Miller, and J. L. Dempsey, Bathochromic Shifts in Rhenium Carbonyl Dyes Induced through Destabilization of Occupied Orbitals, *Inorg. Chem.* **57**, 5389 (2018).
 - (23) L. A. Worl, R. Duesing, P. Chen, L. D. Ciana, and T. J. Meyer, Photophysical properties of polypyridyl carbonyl complexes of rhenium(I), *J. Chem. Soc. Dalt. Trans.* , 849 (1991).
 - (24) K. Ley and K. Schanze, Photophysics of metal-organic π -conjugated polymers, *Coord. Chem. Rev.* **171**, 287 (1998).
 - (25) A. Zarkadoulas, E. Koutsouri, C. Kefalidi, and C. A. Mitsopoulou, Rhenium complexes in homogeneous hydrogen evolution, *Coord. Chem. Rev.* **304–305**, 55 (2015).
 - (26) E. Portenkirchner, S. Schlager, D. Apaydin, K. Oppelt, M. Himmelsbach, D. A. Egbe, H. Neugebauer, G. Knör, T. Yoshida, and N. S. Sariciftci, Using the Alkynyl-Substituted Rhenium(I) Complex (4,4'-Bisphenyl-Ethynyl-2,2'-Bipyridyl)Re(CO)₃Cl as Catalyst for CO₂ Reduction—Synthesis, Characterization, and Application, *Electrocatalysis* **6**, 185 (2015).
 - (27) D. B. MacQueen and K. S. Schanze, Free Energy and Solvent Dependence of Intramolecular Electron Transfer in Donor-Substituted Re(I) Complexes, *J. Am. Chem. Soc.* **113**, 7470 (1991).
 - (28) D. B. MacQueen and K. S. Schanze, Cation-Controlled Photophysics in a Re(I) Fluoroionophore, *J. Am. Chem. Soc.* **113**, 6108 (1991).
 - (29) H. D. Stoeffler, N. B. Thorntor, S. L. Temkin, and K. S. Schanze, Unusual Photophysics of a Rhenium(I) Dipyrrophenazine Complex in Homogenous Solution and Bound to DNA, *J. Am. Chem. Soc.* **117**, 7119 (1995).
 - (30) J. D. Lewis, R. N. Perutz, and J. N. Moore, Proton-controlled photoisomerization: Rhenium(I) tricarbonyl bipyridine linked to amine or azacrown ether groups by a styryl pyridine bridging ligand, *Chem. Commun.* **0**, 1865 (2000).
 - (31) J. D. Lewis, L. Bussotti, P. Foggi, R. N. Perutz, and J. N. Moore, Picosecond forward electron transfer and nanosecond back electron transfer in an azacrown-substituted [(bpy)Re(CO)₃(L)]⁺ complex: Direct observation by time-resolved UV-visible absorption spectroscopy, *J. Phys. Chem. A* **106**, 12202 (2002).
 - (32) A. Gabrielsson, F. Hartl, H. Zhang, J. R. Smith, M. Towrie, A. Viček, and R. N. Perutz, Ultrafast charge separation in a photoreactive rhenium-appended porphyrin assembly monitored by picosecond transient infrared spectroscopy, *J. Am. Chem. Soc.* **128**, 4253 (2006).
 - (33) K. Kiyosawa, N. Shiraishi, T. Shimada, D. Masui, H. Tachibana, S. Takagi, O. Ishitani, D. A. Tryk, and H. Inoue, Electron transfer from the porphyrin S₂ state in a zinc porphyrin-rhenium bipyridyl dyad having carbon dioxide reduction activity, *J. Phys. Chem. C* **113**, 11667 (2009).
 - (34) A. Gabrielsson, F. Hartl, J. R. Lindsay Smith, and R. N. Perutz, Photo-induced ligand substitution at a remote site via electron transfer in a porphyrin-appended rhenium carbonyl supermolecule, *Chem. Commun.* **2**, 950 (2002).
 - (35) Y. Kou, S. Nakatani, G. Sunagawa, Y. Tachikawa, D. Masui, T. Shimada, S. Takagi, D. A. Tryk, Y. Nabetani, H. Tachibana, and H. Inoue, Visible light-induced reduction of carbon dioxide sensitized by a porphyrin-rhenium dyad metal complex on p-type semiconducting NiO as the reduction terminal end of an artificial photosynthetic system, *J. Catal.* **310**, 57 (2014).
 - (36) T. Mutai, J. D. Cheon, S. Arita, and K. Araki, Phenyl-substituted 2,2':6',2''-terpyridine as a new series of fluorescent compounds - Their photophysical properties and fluorescence tuning, *J. Chem. Soc. Perkin Trans. 2* , 1045 (2001).
 - (37) Y. Q. Fang, N. J. Taylor, F. Laverdière, G. S. Hanan, F. Loiseau, F. Nastasi, S. Campagna, H. Nierengarten,

- E. Leize-Wagner, and A. Van Dorsselaer, Ruthenium(II) complexes with improved photophysical properties based on planar 4'-(2-pyrimidinyl)-2,2':6',2''-terpyridine ligands, *Inorg. Chem.* **46**, 2854 (2007).
- (38) K. Hutchison, J. C. Morris, T. A. Nile, J. L. Walsh, D. W. Thompson, J. D. Petersen, and J. R. Schoonover, Spectroscopic and photophysical properties of complexes of 4'-ferrocenyl-2,2':6',2''-terpyridine and related ligands, *Inorg. Chem.* **38**, 2516 (1999).
- (39) D. K. Crites, C. T. Cunningham, and D. R. McMillin, Remarkable substituent effects on the photophysics of Pt(4'-X-trpy)Cl⁺ systems (trpy = 2,2':6',2''-terpyridine), *Inorganica Chim. Acta* **273**, 346 (1998).
- (40) C. Kong, M. Peng, H. Shen, Y. Wang, Q. Zhang, H. Wang, J. Zhang, H. Zhou, J. Yang, J. Wu, and Y. Tian, A novel D-A type terpyridine-based carbazole Zn(II) complex with enhanced two-photon absorption and its bioimaging application, *Dye. Pigment.* **120**, 328 (2015).
- (41) K. Kam-Wing Lo, C. K. Chung, D. Chun-Ming Ng, and N. Zhu, Syntheses, characterisation and photophysical studies of novel biological labelling reagents derived from luminescent iridium(III) terpyridine complexes, *New J. Chem.* **26**, 81 (2002).
- (42) M. Wang, T. Weyhermüller, E. Bill, S. Ye, and K. Wieghardt, Structural and Spectroscopic Characterization of Rhenium Complexes Containing Neutral, Monoanionic, and Dianionic Ligands of 2,2'-Bipyridines and 2,2':6,2-Terpyridines: An Experimental and Density Functional Theory (DFT)-Computational Study, *Inorg. Chem.* **55**, 5019 (2016).
- (43) B. Laramée-Milette, N. Zaccheroni, F. Palomba, and G. S. Hanan, Visible and Near-IR Emissions from κ^2 N- and κ^3 N-Terpyridine Rhenium(I) Assemblies Obtained by an [n×1] Head-to-Tail Bonding Strategy, *Chem. - A Eur. J.* **23**, 6370 (2017).
- (44) E. W. Abel, V. S. Dimitrov, N. J. Long, K. G. Orrell, A. G. Osborne, H. M. Pain, V. Šik, M. B. Hursthouse, and M. A. Mazid, 2,2':6',2''-Terpyridine (terpy) acting as a fluxional bidentate ligand. Part 2. Rhenium carbonyl halide complexes, *fac*-[ReX(CO)₃(terpy)] (X = Cl, Br or I): NMR studies of their solution dynamics, synthesis of *cis*-[ReBr(CO)₂(terp)], *J. Chem. Soc. Dalt. Trans.*, 597 (1993).
- (45) T. Klemens, A. Świtlicka-Olszewska, B. Machura, M. Grucela, H. Janeczek, E. Schab-Balcerzak, A. Szlapa, S. Kula, S. Krompiec, K. Smolarek, D. Kowalska, S. Mackowski, K. Erfurt, and P. Lodowski, Synthesis, photophysical properties and application in organic light emitting devices of rhenium(i) carbonyls incorporating functionalized 2,2':6',2''-terpyridines, *RSC Adv.* **6**, 56335 (2016).
- (46) T. Klemens, A. Świtlicka-Olszewska, B. Machura, M. Grucela, E. Schab-Balcerzak, K. Smolarek, S. Mackowski, A. Szlapa, S. Kula, S. Krompiec, P. Lodowski, and A. Chrobok, Rhenium(i) terpyridine complexes-synthesis, photophysical properties and application in organic light emitting devices, *Dalt. Trans.* **45**, 1746 (2016).
- (47) T. Klemens, K. Czerwińska, A. Szlapa-Kula, S. Kula, A. Świtlicka, S. Kotowicz, M. Siwy, K. Bednarczyk, S. Krompiec, K. Smolarek, S. Maćkowski, W. Danikiewicz, E. Schab-Balcerzak, and B. Machura, Synthesis, spectroscopic, electrochemical and computational studies of rhenium(i) tricarbonyl complexes based on bidentate-coordinated 2,6-di(thiazol-2-yl)pyridine derivatives, *Dalt. Trans.* **46**, 9605 (2017).
- (48) A. M. Blanco-Rodríguez, H. Kvapilová, J. Sýkora, M. Towrie, C. Nervi, G. Volpi, S. Zálaiš, and A. Vlček, Photophysics of Singlet and Triplet Intraligand Excited States in [ReCl(CO)₃(1-(2-pyridyl)-imidazo[1,5- α]pyridine)] Complexes, *J. Am. Chem. Soc.* **136**, 5963 (2014).
- (49) G. E. Shillito, D. Preston, P. Traber, J. Steinmetzer, C. J. McAdam, J. D. Crowley, P. Wagner, S. Kupfer, and K. C. Gordon, Excited-State Switching Frustrates the Tuning of Properties in Triphenylamine-Donor-Ligand Rhenium(I) and Platinum(II) Complexes, *Inorg. Chem.* **59**, 6736 (2020).
- (50) S. Tu, R. Jia, B. Jiang, J. Zhang, Y. Zhang, C. Yao, and S. Ji, Kröhnke reaction in aqueous media: one-pot clean synthesis of 4'-aryl-2,2':6',2''-terpyridines, *Tetrahedron* **63**, 381 (2007).
- (51) L. Sévery, S. Siol, and S. Tilley, Design of Molecular Water Oxidation Catalysts Stabilized by Ultrathin Inorganic Overlayers—Is Active Site Protection Necessary?, *Inorganics* **6**, 105 (2018).
- (52) M. J. Frisch, G. W. Trucks, H. B. Schlegel, G. E. Scuseria, M. A. Robb, J. R. Cheeseman, G. Scalmani, V. Barone, B. Mennucci, G. A. Petersson, H. Nakatsuji, M. Caricato, X. Li, H. P. Hratchian, A. F. Izmaylov, J. Bloino, G. Zheng, J. L. Sonnenberg, M. Hada, M. Ehara, K. Toyota, R. Fukuda, J. Hasegawa, M. Ishida, T. Nakajima, Y. Honda, O. Kitao, H. Nakai, T. Vreven, J. A. Montgomery, J. E. Peralta, F. Ogliaro, M. Bearpark, J. J. Heyd, E. Brothers, K. N. Kudin, V. N. Staroverov, R. Kobayashi, J. Normand, K. Raghavachari, A. Rendell, J. C. Burant, S. S. Iyengar, J. Tomasi, M. Cossi, N. Rega, J. M. Millam, M. Klene, J. E. Knox, J. B. Cross, V. Bakken, C. Adamo, J. Jaramillo, R. Gomperts, R. E. Stratmann, O. Yazyev, A. J. Austin, R. Cammi, C. Pomelli, J. W. Ochterski, R. L. Martin, K. Morokuma, V. G. Zakrzewski, G. A. Voth, P. Salvador, J. J. Dannenberg, S. Dapprich, A. D. Daniels, Farkas, J. B. Foresman, J. V. Ortiz, J. Cioslowski, and D. J. Fox, Gaussian 09, Revision D.01 (2009).
- (53) J. K. Hino, L. D. Ciana, W. J. Dressick, and B. P. Sullivan, Substituent constant correlations as predictors of spectroscopic, electrochemical, and photophysical properties in ring-substituted 2,2'-bipyridine complexes of rhenium(I), *Inorg. Chem.* **31**, 1072 (1992).
- (54) T. Lu and F. Chen, Multiwfn: A multifunctional wavefunction analyzer, *J. Comput. Chem.* **33**, 580 (2012).
- (55) P. Hamm, M. Lim, and R. M. Hochstrasser, Vibrational energy relaxation of the cyanide ion in water, *J. Chem. Phys.* **107**, 10523 (1997).
- (56) P. Hamm, R. A. Kaindl, and J. Stenger, Noise suppression in femtosecond mid-infrared light sources, *Opt. Lett.* **25**, 1798 (2000).
- (57) J. Helbing and P. Hamm, Compact implementation of Fourier transform two-dimensional IR spectroscopy without phase ambiguity, *J. Opt. Soc. Am. B* **28**, 171 (2011).
- (58) S. Sato, Y. Matubara, K. Koike, M. Falkenström, T. Katayama, Y. Ishibashi, H. Miyasaka, S. Taniguchi, H. Chosrowjan, N. Mataga, N. Fukazawa, S. Koshi-

- hara, K. Onda, and O. Ishitani, Photochemistry of *fac*-[Re(bpy)(CO)₃Cl], Chem. - A Eur. J. **18**, 15722 (2012).
- (59) J. Bredenbeck, J. Helbing, and P. Hamm, Continuous scanning from picoseconds to microseconds in time resolved linear and nonlinear spectroscopy, Rev. Sci. Instrum. **75**, 4462 (2004).
- (60) G. E. Shillito, T. B. Hall, D. Preston, P. Traber, L. Wu, K. E. Reynolds, R. Horvath, X. Z. Sun, N. T. Lucas, J. D. Crowley, M. W. George, S. Kupfer, and K. C. Gordon, Dramatic Alteration of ³ILCT Lifetimes Using Ancillary Ligands in [Re(L)(CO)₃(phen-TPA)]ⁿ⁺ Complexes: An Integrated Spectroscopic and Theoretical Study, J. Am. Chem. Soc. **140**, 4534 (2018).
- (61) A. Kumar, S.-S. Sun, and A. J. Lees, Photophysics and Photochemistry of Organometallic Rhenium Dimine Complexes, in *Photophysics of Organometallics*, edited by A. J. Lees (Springer Berlin Heidelberg, Berlin, Heidelberg, 2010) pp. 37–71.
- (62) F. P. A. Johnson, M. W. George, F. Hartl, and J. J. Turner, Electrocatalytic Reduction of CO₂ Using the Complexes [Re(bpy)(CO)₃L]ⁿ (n = +1, L=P(OEt)₃, CH₃CN; n=0, L=Cl⁻, Otf⁻; bpy=2,2'-Bipyridine; Otf⁻=CF₃SO₃⁻) as Catalyst Precursors: Infrared Spectroelectrochemical Investigation, Organometallics **15**, 3374 (1996).
- (63) B. Probst, C. Kolano, P. Hamm, and R. Alberto, An efficient homogeneous intermolecular rhenium-based photocatalytic system for the production of H₂, Inorg. Chem. **48**, 1836 (2009).
- (64) B. Probst, A. Rodenberg, M. Guttentag, P. Hamm, and R. Alberto, A highly stable rhenium-cobalt system for photocatalytic H₂ production: Unraveling the performance-limiting steps, Inorg. Chem. **49**, 6453 (2010).
- (65) C. Bachmann, B. Probst, M. Guttentag, and R. Alberto, Ascorbate as an electron relay between an irreversible electron donor and Ru(II) or Re(I) photosensitizers, Chem. Commun. **50**, 6737 (2014).
- (66) A. Horváth and K. L. Stevenson, Transition metal complex exciplexes, Coord. Chem. Rev. **153**, 57 (1996).
- (67) A. Vogler and H. Kunkely, Charge transfer exciplex emission involving a transition metal complex, Inorganica Chim. Acta **45**, L265 (1980).

FOR TABLE OF CONTENTS ONLY



A series of Re(I) tricarbonyl complexes with 4'-(4-substituted-phenyl)-terpyridine ligands bearing substituents of different electron donating abilities were evaluated. Substituents ranging from CN to OMe lead to complexes with short-lived $^3\text{MLCT}$ excited states, whose properties are largely correlated to the Hammett σ_p substituent constants. In contrast, the complex with a strongly donating NMe₂ substituent has a long-lived $^3\text{ILCT}$ state which can drive light-induced hydrogen evolution with a Cobalt-based catalyst.